

# Resonance-like piezoelectric electron-phonon interaction in layered structures

B. A. Glavin, V.A. Kochelap, and T.L. Linnik  
*V. E. Lashkarev Institute of Semiconductor Physics,  
Pr. Nauki 41, Kiev 03028, Ukraine*

A.J. Kent, N.M. Stanton, and M. Henini  
*School of Physics and Astronomy, University of Nottingham, Nottingham NG7  
2RD UK.*

We show that mismatch of the piezoelectric parameters between layers of multiple-quantum well structures leads to modification of the electron-phonon interaction. In particular, short-wavelength phonons propagating perpendicular to the layers with wavevector close to  $2\pi n/d$ , where  $d$  is the period of the structure, induce a strong smoothly-varying component of the piezo-potential. As a result, they interact efficiently with 2D electrons. It is shown, that this property leads to emission of collimated quasi-monochromatic beams of high-frequency acoustic phonons from hot electrons in multiple-quantum well structures. We argue that this effect is responsible for the recently reported monochromatic transverse phonon emission from optically excited GaAs/AlAs superlattices, and provide additional experimental evidences of this.

## I. INTRODUCTION

It is now well-established that the properties of acoustic phonons in layered structures can be very different from those in bulk crystals: mismatch of the elastic properties of the layers results in formation of a folded phonon spectrum and phonon stop-bands, etc. In particular, this leads to the reduction of the momentum-conservation restrictions for Raman scattering of light, which allows probing of the folded acoustic phonons by light-scattering methods (see Ref. 1 for review). In this communication we show that a similar effect takes place for piezoelectric electron-acoustic phonon interactions in layered structures due to mismatch of the piezo-parameters of the quantum-well and barrier layers. The effect is especially pronounced for phonons propagating close to the structure axis and whose wavevector is about  $2\pi n/d$ , where  $d$  is the structure period. In the following, we will call such phonons *resonant*. We show that the enhanced interaction strongly affects hot-carrier relaxation in multiple-quantum well (MQW) structures. Namely, *spontaneous* emission of collimated quasi-monochromatic beams of high-frequency phonons by hot electrons becomes possible. This is in contrast with *stimulated* emission of phonons where their monochromatic character is set due to nonlinear electron-phonon dynamics in a system with population inversion.<sup>2</sup> We argue that recent observation of monochromatic transverse acoustic phonon emission in GaAs/AlAs multilayered structures<sup>3</sup> can be attributed to the considered modification of the piezoelectric electron-phonon interaction. We report also new experimental results that support this interpretation.

## II. PHONON-INDUCED PIEZOELECTRIC POTENTIAL IN MULTILAYERED STRUCTURES

To begin, we recall briefly the main features of electron-acoustic phonon interaction in solitary quantum wells (QW) (see, for example, Ref. 4). The probability of the electron intra-subband transitions is proportional to the form-factor,  $J$ , given by

$$J \sim \left| \int dz \chi^2(z) \varphi \right|^2, \quad (1)$$

where  $\chi$  is envelope wavefunction of confined electron and  $\varphi$  is the phonon-induced perturbation potential. In a uniform medium, phonons are plane waves and the same applies to  $\varphi$ . Thus,  $\varphi \sim \exp(iq_z z)$ , where  $\mathbf{q}$  is the phonon wavevector and the  $z$ -axis is directed perpendicular to the layers. As a result, for  $q_z \gg 1/d_{QW}$ , where  $d_{QW}$  is the QW width, the form-factor is small and electron-phonon interaction is suppressed. On the other hand, interaction with phonons of large in-plane wavevector is prohibited as well, due to in-plane momentum conservation. These factors suppress interaction of electrons with high-frequency acoustic phonons. This holds for both the deformation potential and piezoelectric interaction mechanisms.

In multi-layered systems, e.g. MQW heterostructures, the situation is essentially different. The MQW structure is shown schematically in Fig.1. The QW and barrier width are  $d_{QW}$  and  $d_B$  respectively, and the MQW period is  $d = d_{QW} + d_B$ . With no tunneling coupling between the adjacent QWs, the properties of electrons are identical to those in a solitary QW. On the other hand, the phonons are modified due to mismatch of the *elastic* properties in the QW and the barrier layers. However, for typical MQW structures this mismatch is small and moderate modifications are noticeable only in small regions of phonon momentum space corresponding to Bragg reflections of phonons. This has very little effect on the overall electron-phonon interaction. However, as we shall see below, mismatch of the *piezoelectric* parameters, while having negligible effect on the phonon mode structure, modifies the interaction potential  $\varphi$ . The latter is determined by equation

$$\nabla^2 \Phi = \frac{1}{\epsilon \epsilon_0} \nabla \cdot \mathbf{P}. \quad (2)$$

Here  $\epsilon$  is the dielectric permittivity and  $\epsilon_0$  the absolute dielectric constant.  $\mathbf{P}$  is the polarization induced due to the piezoelectric effect:  $P_i = e_{ijk} u_{jk}$ , where  $u_{jk}$  is strain tensor and  $e_{ijk}$  are piezo-constants. For the case of strain induced by acoustic phonons of wavevector  $\mathbf{q} = \{q_x, q_y, q_z\}$ , the potential can be expressed as  $\Phi = \phi(z) \exp(i(q_x x + q_y y))$ , and the equation for  $\phi$  is

$$\frac{d^2 \phi}{dz^2} - q_{\parallel}^2 \phi = R(z) \exp(iq_z z), \quad (3)$$

where  $q_{\parallel} = \sqrt{q_x^2 + q_y^2}$  and  $R$  is periodic function:  $R(z) = R(z + d)$ . The periodicity of  $R$  is due to the piezoelectric parameters mismatch in the QW and barrier layers. The specific form of  $R$  depends on the crystal structure of the materials which constitute the MQW and also the phonon wavevector and polarization. It is convenient to expand  $R(z)$  as a Fourier series

$$R(z) = \sum_{n=-\infty}^{\infty} R_n \exp(iq_0 n z), \quad q_0 = 2\pi/d. \quad (4)$$

Then, the solution of Eq. (3) is

$$\phi = -\exp(iq_z z) \sum_{n=-\infty}^{\infty} \frac{R_n \exp(iq_0 n z)}{(q_z + q_0 n)^2 + q_{\parallel}^2}. \quad (5)$$

We see that, for  $q_z \approx -q_0 n$ , the potential has a component which is smooth function of  $z$ . As a result, the form-factor for such  $q_z$  is not suppressed, even if  $q_z a \gg 1$ . Furthermore, for small  $q_{\parallel}$  the amplitude of the smoothly-varying component is large. Therefore, the role of mismatch of the piezo-constants is important for resonant phonons which propagate close to the MQW axis.

Particular characteristics of the piezoelectric interaction are determined by the coefficients  $R_n$ . It is convenient to present them in the following form:

$$R_0 = -q^2 \frac{e\bar{e}}{\epsilon \epsilon_0}, \quad (6)$$

$$R_n = i \frac{e\bar{\delta e} q}{\epsilon \epsilon_0 d} (1 - \exp(-iq_0 n d_B)), \quad n \neq 0.$$

Here  $e$  is elementary electric charge and  $\bar{e}$  and  $\bar{\delta e}$  are characteristic piezo-constants, which depend on the direction and polarisation of phonon. Note that in Eq. (6) and subsequent equation (8) we assume that the amplitude of the displacement for a phonon is unity). We now consider in detail the example of a GaAs/AlAs MQW structure with its growth axis parallel to (001) crystal axis. The structures are composed of cubic-symmetry materials and the piezoelectric properties are characterized by the only nonvanishing coefficient,  $e_{14}$ . Using the isotropic elastic model we obtain for longitudinal, transverse vertical and transverse horizontal phonons the following expressions:

$$\bar{e}^{(LA)} = \frac{1}{2} \sin^2 \theta \cos \theta \sin 2\phi_{ph} \left( e_{14} + \frac{d_B}{d} \delta e_{14} \right), \quad (7)$$

$$\bar{\delta e}^{(LA)} = \delta e_{14} \sin^2 \theta \sin 2\phi_{ph} \left( 1 + \frac{3q \cos \theta}{q_0 n} \right),$$

$$\begin{aligned}
\bar{e}^{(TA,v)} &= \sin \theta \cos^2 \theta \sin 2\phi_{ph} \left( e_{14} + \frac{d_B}{d} \delta e_{14} \right), \\
\bar{\delta e}^{(TA,v)} &= \delta e_{14} \sin \theta \cos \theta \sin 2\phi_{ph} \left( 1 + \frac{2q \cos \theta}{q_0 n} \right), \\
\bar{e}^{(TA,h)} &= 2 \sin \theta \cos \theta \cos 2\phi_{ph} \left( e_{14} + \frac{d_B}{d} \delta e_{14} \right), \\
\bar{\delta e}^{(TA,h)} &= \delta e_{14} \sin \theta \cos 2\phi_{ph} \left( 1 + \frac{2q \cos \theta}{q_0 n} \right).
\end{aligned}$$

Here  $e_{14}$  is the piezo-constant in the QW,  $\delta e_{14}$  is the mismatch of the piezo-constants in the barrier and the QW, and  $\theta$ ,  $\phi_{ph}$  are spherical angles of the phonon wavevector. The polarizations of transverse phonons are defined such that the displacement for the horizontally polarized phonon is parallel to the layers of the MQW, and for the vertically polarized phonon it lies in the plane formed by the wavevector and the normal to the layers. It is straightforward to obtain from these equations that close to resonance,  $q_z = -q_0 n + \delta q_z$ ,  $\delta q_z \ll |q_0 n|$ , and for small in-plane wavevector, the major mismatch contribution is due to the transverse phonons, whose form-factors are

$$\begin{aligned}
J^{(TA,h)} &\approx 4 \frac{e^2 \delta e_{14}^2}{\epsilon^2 \epsilon_0^2 d^2} \sin^2 \frac{q_0 n d_B}{2} \cos^2 2\phi_{ph} \frac{q_{\parallel}^2}{(\delta q_z^2 + q_{\parallel}^2)^2}, \\
J^{(TA,v)} &\approx 4 \frac{e^2 \delta e_{14}^2}{\epsilon^2 \epsilon_0^2 d^2} \sin^2 \frac{q_0 n d_B}{2} \sin^2 2\phi_{ph} \frac{q_{\parallel}^2}{(\delta q_z^2 + q_{\parallel}^2)^2}.
\end{aligned} \tag{8}$$

As we see, the form-factor dependence on  $q_z$  has a shape of a peak. As  $q_{\parallel}$  decreases, the width of the peak decreases and its height increases. This is illustrated in Fig. 2, where we plot the form-factor for transverse phonons of vertical polarization and  $\phi_{ph} = \pi/4$  as a function of  $q_z$  for  $q_{\parallel} = 10^7 \text{ m}^{-1}$  and  $10^8 \text{ m}^{-1}$  (all form-factors are plotted for  $d_{QW} = 6 \text{ nm}$ ,  $d_B = 2 \text{ nm}$  and normalized to its value for  $q_z = 0$ ; and the form-factor of transverse phonons of horizontal polarization is similar to that of phonons of horizontal polarizations). For comparison, the form-factor for a plane-wave potential is shown in the figure as well. The numbers near the peaks, corresponding to  $q_{\parallel} = 10^7 \text{ m}^{-1}$  indicate the amplitudes of the peak.

It should be mentioned that the described features hold provided the number of periods in MQW structure,  $N$ , is big enough. Indeed, as can be shown from the solution of Poisson's equation for finite- $N$  structure, the resonances are pronounced if  $q_{\parallel} N d > 1$ .

These properties of the form-factor allow us to suggest that 2D hot electrons confined in the QWs of MQW structure can emit quasi-monochromatic collimated beams of acoustic phonons. To prove this, we performed calculations of the phonon emission for the experimental setup, which allows to register the resonant phonons, see Fig. 3a. In this case the emitted phonons are registered by the superconducting bolometer deposited on the back side of the substrate. Typically, the MQW and bolometer lateral dimensions are much less than the thickness of the substrate. Therefore, the bolometer probes only phonons propagating close to the MQW axis.

The results for the spectrum of the phonon emission  $Q$  are shown in Fig. 4.  $Q$  is determined as the phonon power emitted per MQW period per unit area and per unit frequency interval. The calculations were performed for a GaAs/AlAs MQW where the angle between the phonon wavevector and MQW axis is restricted by the value  $\theta_{max} = 0.1$  (roughly,  $2\theta_{max}$  can be estimated as the ratio of MQW lateral dimensions to the substrate thickness). We used the following material parameters: density  $\rho = 5316 \text{ kg/m}^3$ , longitudinal and transverse sound velocities  $s_l = 4730 \text{ m/s}$ ,  $s_t = 3345 \text{ m/s}$ , respectively,  $e_{14} = -0.16 \text{ C/m}^2$ ,  $\delta e_{14} = -0.065 \text{ C/m}^2$ , and  $\epsilon = 12.9$ . These data were taken from Ref. 5. The temperature of hot electrons was assumed to be  $100\text{K}$ , and the QW and barrier width are  $d_B = 6 \text{ nm}$  and  $d_B = 2 \text{ nm}$ . The electron envelope wavefunctions correspond to confinement in an infinitely deep rectangular QW. As it was expected, the emission spectrum of the transverse phonons has sharp peaks for resonant phonon frequencies. For longitudinal phonons, the contribution of resonant piezoelectric interaction is very much weaker. Therefore, it cannot be resolved on the broad-spectrum deformation-potential contribution (in calculations we used deformation potential constant  $8 \text{ eV}$ ). Note, that in experiments the quasi-monochromatic transverse phonon signal and broad-spectrum longitudinal-phonon signal can be resolved based on the different travel times necessary to reach the bolometer.

### III. COMPARISON WITH EXPERIMENTAL RESULTS

Recently, monochromatic longitudinal and transverse phonon emission was observed under the femtosecond laser excitation of electrons in GaAs/AlAs MQW.<sup>6,3</sup> In these experiments the coherent nature of longitudinal phonons was detected by high-frequency modulation of the optical reflection using the pump-probe technique. Complementary measurements of the emitted phonon spectral distribution was accomplished using the phonon filtering method. In addition to conventional structures, Fig. 2a, “filtered” samples were manufactured, where an additional, mirror, superlattice was grown between the “generator” superlattice and the bolometer. The parameters of the mirror superlattice were selected such that its stop-bands match the mini-Brillouin zone-center phonon frequencies of the generator superlattice. Then, the phonon signals for different excitation photon energies, below and above the fundamental edge of superlattice, were measured. In the structures without a filter, a pronounced increase of the phonon signal with increase of the photon energy was observed, which corresponds to the onset of light absorption in superlattice. In contrast, for the filtered samples no such increase was observed for both longitudinal and transverse phonons. This suggests quasi-monochromatic character of the emitted phonon spectrum. For longitudinal phonons this result can be attributed to the impulsive stimulated Raman scattering,<sup>7</sup> which is supported by the observation of the reflectance modulation at frequency corresponding to the phonon-miniband center longitudinal phonons. However, no such modulation is present at the corresponding transverse-phonon frequency. The only remaining possibility is that monochromatic transverse phonons are emitted under the relaxation of nonequilibrium carriers following the femtosecond pulse. However, conventional mechanisms of electron-phonon interaction do not provide such sharp phonon spectral features. We believe that the observed monochromatic transverse phonon emission could be attributed to the resonant piezoelectric-mismatch-induced interaction mechanism proposed in this paper. Note, however, that the results of the numerical calculations presented here can not be used for quantitative estimate of the phonon emission power in these experiments. This is because of complicated relaxation pattern of electrons and holes in superlattices excited by ultrafast pulses.

The new results described here concern the angle dependence of the emission. These were obtained using the phonon imaging technique<sup>8</sup> in which the laser spot is scanned across the generator SL, thus changing its position relative to the detector. We used two SL structures grown by MBE on 0.35 mm-thick semi-insulating GaAs substrates. Sample A contained just a generator SL and Sample B contained the generator SL and a filter SL. The generator consisted of 40 periods, each of 22 monolayers (ML) of GaAs and 4 ML of AlAs. For these SL parameters, the first mini-Brillouin zone-centre TA phonon frequency is 450 GHz. In Sample B, the notch filter was grown below the generator. It consisted of 40 periods, each of 7 ML GaAs and 7 ML AlAs, and was separated from the generator SL by a 0.5 micron-thick GaAs spacer layer. The first mini-Brillouin zone-boundary stop band of the filter is coincident with the generator frequency and prevents 450 GHz phonons reaching the detector (bolometer) on the rear face of the substrate. Using this arrangement, we previously showed that, when the generator SL was resonantly excited by 100 femtosecond laser pulses, monochromatic TA phonons of frequency 450 GHz were generated<sup>3</sup>.

Bolometer signals for on- and off-resonance photoexcitation of the generator SL in Sample A are shown in Fig. 5. In this case the laser spot is located directly opposite the detector. The off-resonance case corresponds to the photon energy below the fundamental edge in superlattice but above that in bulk GaAs. Here, the bolometer response is due to ballistic and diffusive phonons generated via relaxation of the photoexcited carriers in GaAs. The on-resonance case corresponds to the photon energy above the fundamental edge in the superlattice. Therefore, the increase in signal under resonant photoexcitation is due to phonon emission from carrier relaxation in the superlattice, including quasi-monochromatic (450 GHz) phonons. In the angle dependence measurements, we display the difference between the on- and off-resonance signals at times close to the ballistic time of flight for TA phonons (indicated by the dashed lines in Fig. 5). Fig. 6 shows the full 2D image for Sample B (filtered). The pattern is very similar to the TA phonon focussing pattern in cubic GaAs, convolved with the sizes of the laser spot (about 40 microns-diameter) and the detector (40 x 40 microns squared). Linescans, taken horizontally through the centre of the images (as indicated by the dashed line in Fig. 7), for Sample A and Sample B are shown in Fig. 7, and clearly show the difference in the angle dependence of the emission. It is observed that in the case of the unfiltered sample (A) the emission is directed into a narrower range of angles. This suggests that the monochromatic (450 GHz) component of the TA signal is emitted in a direction close to the SL growth direction as predicted by the theory. Taking account of the size of the source and detector and also phonon focussing effects, we can estimate an upper limit for the angle to the SL normal at which the monochromatic phonons are emitted to be about 10 degrees.

The reported experiments are for femtosecond pulsed optical excitation of the generator SL. From the above theoretical considerations it follows that quasi-monochromatic transverse phonons can be emitted under long-pulse excitation as well. The corresponding measurements are currently in progress and they will be reported elsewhere.

## IV. CONCLUSIONS

In conclusion, we have demonstrated that mismatch of the piezoelectric constants in the quantum well and barrier layers of multiple quantum well structures leads to resonance-like enhancement of piezoelectric electron-phonon interaction for phonons propagating close to the structure axis and having wavevector close to  $2\pi n/d$ . This gives rise to the emission of quasi-monochromatic phonon beams by hot electrons. We suggest that this behaviour can account for the recent observation of monochromatic transverse phonon emission in GaAs/AlAs multiple quantum well structures. Presented in this paper supplementary measurements of the angle-dependence of the transverse phonon emission support this interpretation.

The availability of a source of monochromatic high-frequency transverse phonons can enhance the applicability of phonon-spectroscopy methods. As we have shown, the piezoelectric MQW structures are able to emit such phonons, potentially, even with the use of relatively simple laser excitation technique.

We would like to note also that the resonant contribution to piezoelectric electron-phonon interaction considered here may play essential role in various vertical transport phenomena in semiconductor superlattice structures.

## ACKNOWLEDGMENTS

This work was supported by Royal Society of the UK. BAG and VAK also acknowledge partial support under the STCU grant #3922.

---

<sup>1</sup> B. Jusserand, and M. Cardona, in *Light Scattering in Solids V*, edited by M. Cardona and G. Güntherodt (Springer, Berlin, 1989).

<sup>2</sup> A.J. Kent, R.N. Kini, N.M. Stanton, M. Henini, B.A. Glavin, V.A. Kochelap, and T.L. Linnik, Phys. Rev. Lett., to be published.

<sup>3</sup> N.M. Stanton, R.N. Kini, A.J. Kent, and M. Henini, Phys. Rev. B **69**, 125341 (2004).

<sup>4</sup> P.J. Price, Solid State Commun. **51**, 607 (1984); Surf. Sci. **143**, 145 (1984).

<sup>5</sup> O. Madelung, *Semiconductors: Data Handbook* (Springer, Berlin, 2004).

<sup>6</sup> N.M. Stanton, R.N. Kini, A.J. Kent, M. Henini, and D. Lehmann, Phys. Rev. B **68**, 113302 (2003).

<sup>7</sup> R. Merlin, Solid State Commun. **102**, 207 (1997).

<sup>8</sup> J P Wolfe, *Imaging Phonons: Acoustic Wave Propagation in Solids* (Cambridge University Press, Cambridge, 1998).

FIG. 1. Schematics of MQW structure. Electrons are confined in QW layers with envelope wavefunction  $\chi$ . The QW and barrier layers are characterized by individual values of piezoelectric parameters,  $\{e^{(QW)}\}$  and  $\{e^{(B)}\}$ .

FIG. 2. Form-factors of electron-phonon interaction as a function of  $z$ -component of the phonon wavevector of transverse phonons of vertical polarization for two values of the in-plane wavevector. For reference, the form-factor of the plane-wave potential is provided. All form-factors are normalized to its value for  $q_z = 0$ .

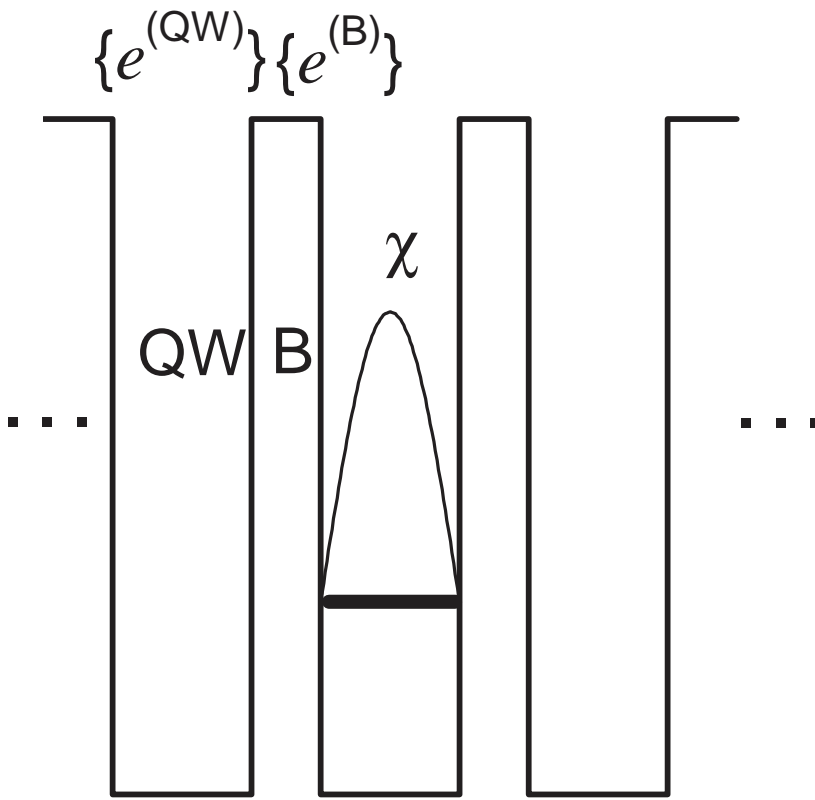
FIG. 3. (a) Schematics of the for measuring phonon emission form the multiple quantum well structures. The phonon signal is registered by the superconducting bolometer deposited on the back side of the substrate. (b) Similar structure but with additional filter superlattice reflecting phonons in narrow frequency bands.

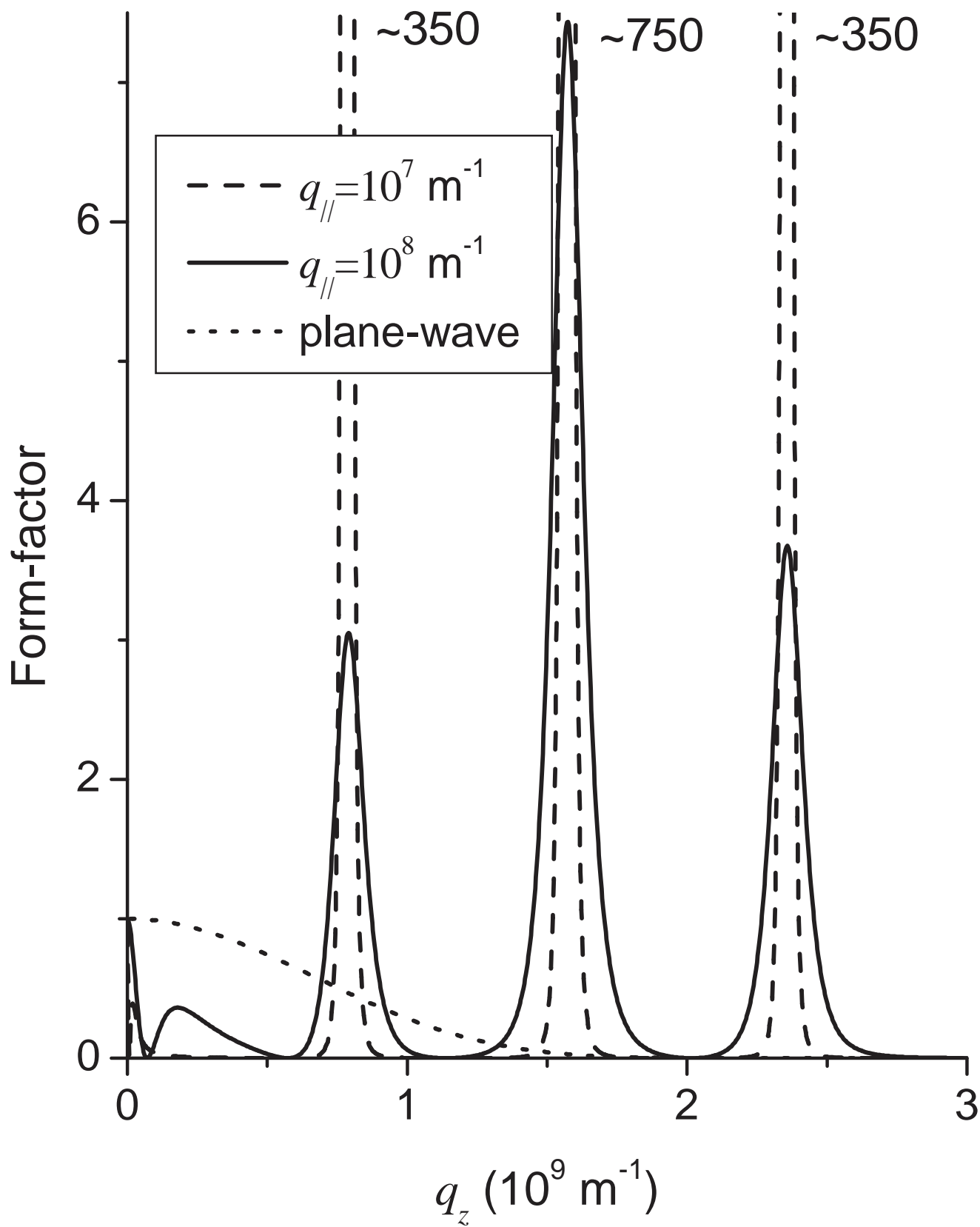
FIG. 4. The phonon emission spectrum of GaAs/AlAs MQW structure for transverse (solid line) and longitudinal (dashed line) phonons. The values of the angle between the emitted phonon wavevector and the MQW axis are restricted by  $\theta_{max} = 0.1$ . The electron temperature is  $100K$ .

FIG. 5. Bolometer signals for on- and off-resonance optical pumping of sample A. The large peak is due to transverse phonons. The time gate used for the measurements of the angle dependence of TA intensity is indicated.

FIG. 6. Phonon image of sample B (difference between on- and off-resonance phonon intensities). The numbers indicate position of the laser spot with respect to bolometer in millimeters. The horizontal dashed line show the axis of the linescans displayed in Fig. 7.

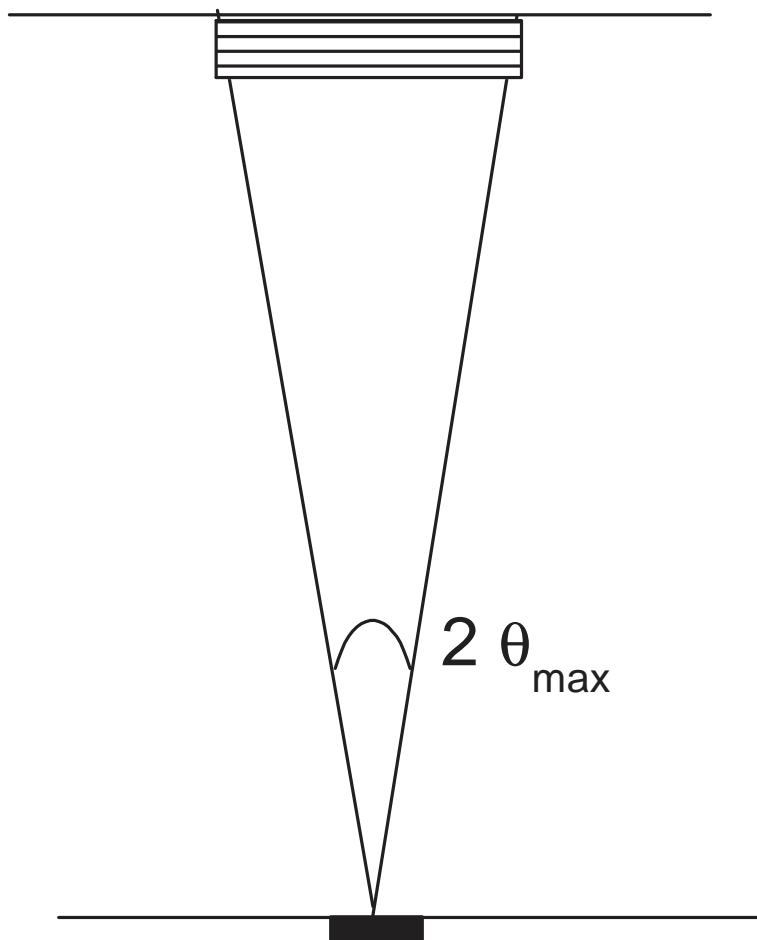
FIG. 7. Linescans of the TA intensity as a function of emission angle for samples A and B.





**a**

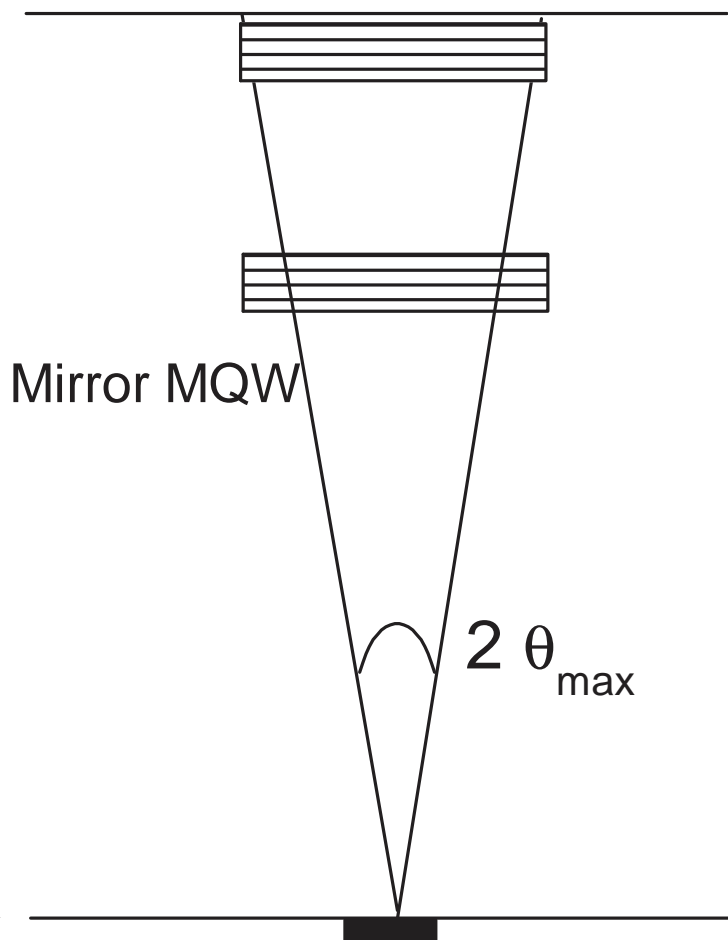
Active MQW



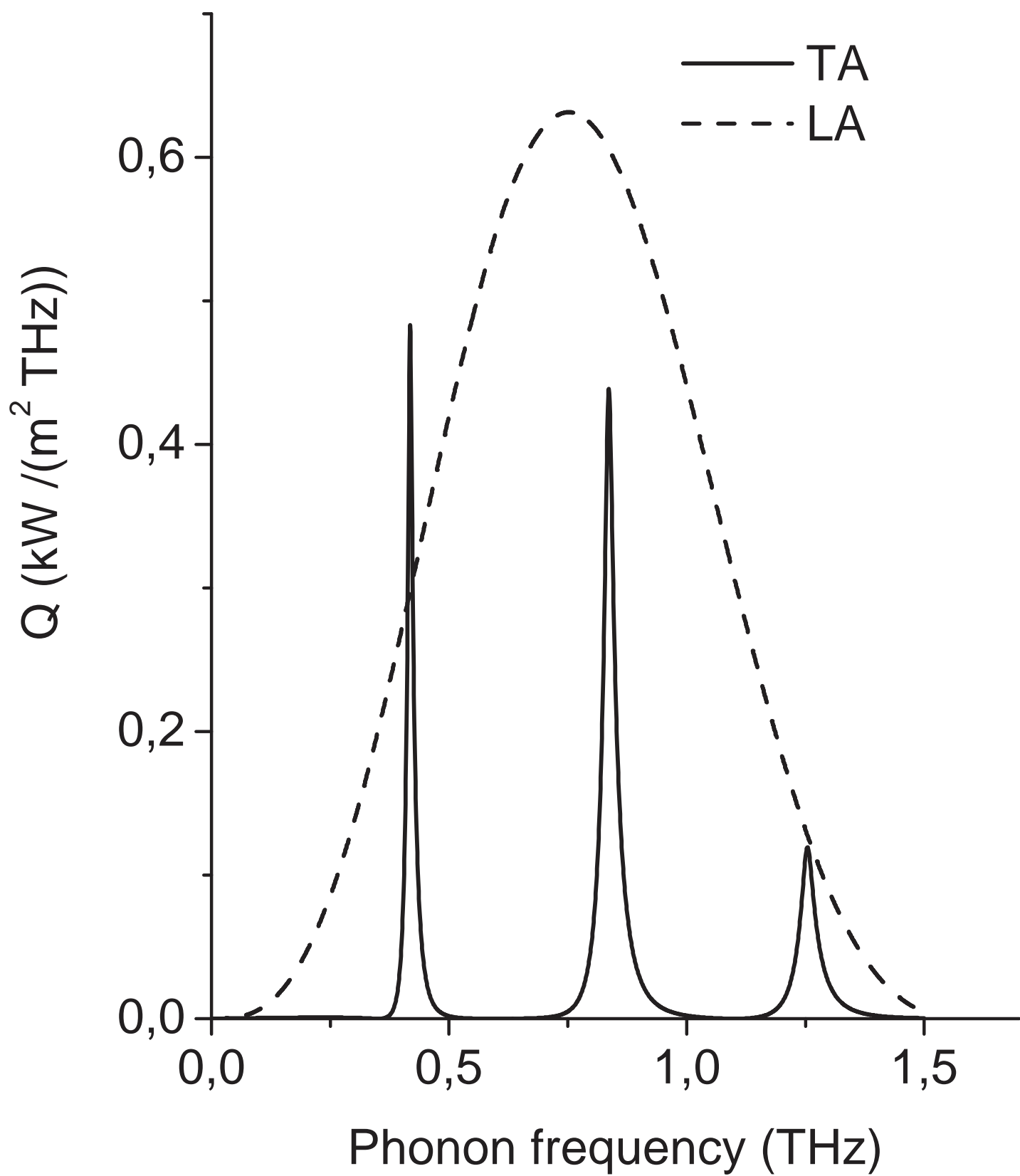
Bolometer

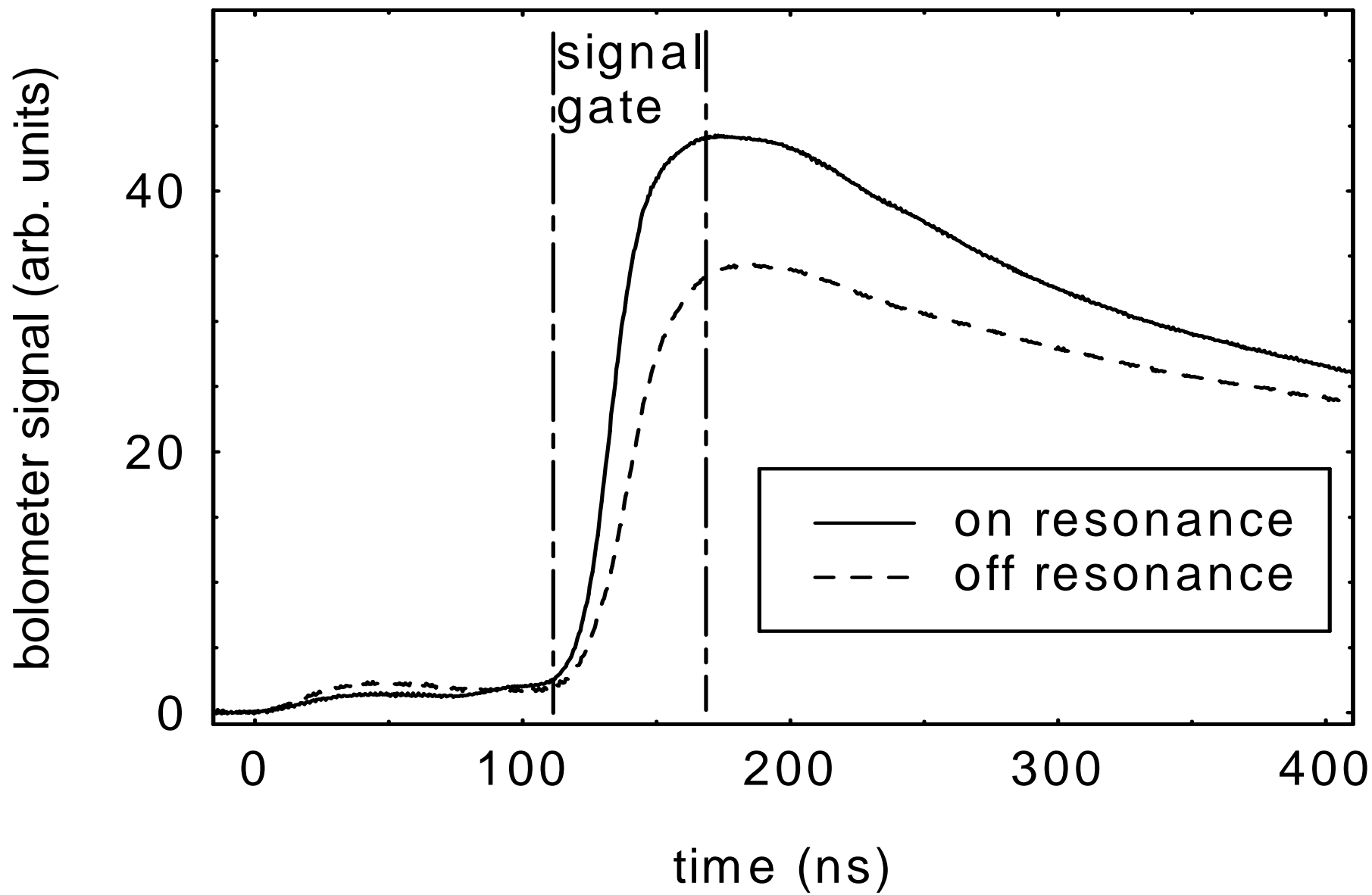
**b**

Active MQW



Bolometer





max



min

